Somato-dendritic nicotinic receptor responses recorded *in vitro* from the medial septal diagonal band complex of the rodent

Zaineb Henderson[1], András Boros[2], Gergely Janzso[3], Andrew J. Westwood[1], Hannah Monyer[4] and Katalin Halasy[3]

[1]*School of Biomedical Sciences, University of Leeds, Leeds LS2 9JT, UK*
[2]*Gedeon Richter Ltd, Gyömröi u. 24, 1475, Budapest, Hungary*
[3]*Department of Anatomy and Histology, Faculty of Veterinary Science, Szent István University, István u.2, 1078, Budapest, Hungary*
[4]*Department of Clinical Neurobiology, Interdisciplinary Centre for Neuroscience, University of Heidelberg, 69120 Heidelberg, Germany*

The medial septal diagonal band area (MS/DB), made up of GABAergic and cholinergic neurones, plays an essential role in the generation and modulation of the hippocampal theta rhythm. To understand the part that the cholinergic neurones might play in this activity, we sought to determine whether postsynaptic nicotinic receptor responses can be detected in slices of the rodent MS/DB by puffing on acetylcholine (ACh). Neurones were characterized electrophysiologically into GABAergic and cholinergic neurones according to previous criteria. Responses of the MS/SB neurones to ACh were various combinations of fast depolarizations (1.5–2.5 s), fast hyperpolarizations (3–4 s) and slow depolarizations (20–30 s), the latter two being blocked by atropine. The fast depolarizations were partially or not blocked with cadmium and low calcium, tetrodotoxin, and antagonists of other ionotropic receptors, and were antagonized with 25 μM mecamylamine. Pharmacological investigation of the responses showed that the $\alpha7^*$ nicotinic receptor type is associated with cholinergic neurones and 10% of the GABAergic neurones, and that non$\alpha7^*$ nicotinic receptor subtypes are associated with 50% of the GABAergic neurones. Pharmacological dissection of evoked and spontaneous postsynaptic responses, however, did not provide evidence for synaptic nicotinic receptor transmission in the MS/DB. It was concluded that nicotinic receptors, although prevalent on the somatic and/or dendritic membrane compartments of neurones in the MS/DB, are on extrasynaptic sites where they presumably play a neuromodulatory role. The presence of $\alpha7^*$ nicotinic receptors on cholinergic neurones may also render these cells specifically vulnerable to degeneration in Alzheimer's disease.

(Received 17 June 2004; accepted after revision 2 November 2004; first published online 4 November 2004)
Corresponding author Z. Henderson: School of Biomedical Sciences, Worsley Building, University of Leeds, Leeds LS2 9JT, UK. Email: z.henderson@leeds.ac.uk

The medial septal diagonal band area (MS/DB) is believed to play a pivotal role in the generation and pacing of theta frequency (4–12 Hz) oscillations in the hippocampus (reviewed by Stewart & Fox, 1990). The predominant neuronal populations in the MS/DB are cholinergic and GABAergic cells, and a proportion of the latter are parvalbumin containing (Panula *et al.* 1984; Brashear *et al.* 1986; Freund, 1989). Both the cholinergic and GABAergic cells, including those that contain parvalbumin, project to the hippocampus via the dorsal fornix/fimbria pathway (Lewis *et al.* 1967; Kohler *et al.* 1984; Amaral & Kurz, 1985; Freund, 1989). The septo-hippocampal GABAergic cells, which have myelinated axons, innervate the somata and dendrites of GABAergic hippocampal interneurones, while the cholinergic neurones have unmyelinated axons and synapse onto all hippocampal cell types (Frotscher & Leranth, 1985; Freund & Antal, 1988; Jones *et al.* 1999; Henderson *et al.* 2001). These contrasting features of GABAergic and cholinergic neurones suggest that they may have differing functions in the generation or maintenance of hippocampal theta activity.

Septo-hippocampal neurones *in vivo* display a rhythmic bursting firing that is tightly coupled to the frequency of the hippocampal theta rhythm (Green & Arduini, 1954;

This work is dedicated to the memory of Professor E. H. Buhl.

 DOI: 10.1113/jphysiol.2004.070300

Dutar *et al.* 1986; Alonso *et al.* 1987; Sweeney *et al.* 1992), and this activity is displayed by both cholinergic and GABAergic neurones (Brazhnik & Fox, 1997, 1999; King *et al.* 1998). The mechanisms for the generation and phase-locking of the rhythmic burst firing, and how these activities contribute to the generation of the hippocampal theta rhythm are still not entirely understood. The role played by the local circuitry of the MS/DB GABAergic and cholinergic neurones in the generation of theta frequency activity is also unexplored. The cholinergic neurones have the potential to provide both fast nicotinic and slow muscarinic receptor-based synaptic activity, and thus to take the place of glutamatergic neurones in the generation and synchronization of rhythmic activity in the MS/DB. Cholinergic synapses and local collaterals of cholinergic neurones have been described in the MS/DB by electron microscopical methods (Bialowas & Frotscher, 1987; Leranth & Frotscher, 1989; Milner, 1991; Henderson *et al.* 2001), making this possibility plausible. The aim of this study therefore was to determine whether fast cholinergic transmission is a feature of the MS/DB.

Methods

Preparation of brain slices

All experiments were performed in accordance with the UK Animals (Scientific Procedures) Act 1986. Male Wistar rats (16–21 days postnatal; 30–60 g, $n = 84$), and male or female C57BL/6 transgenic mice with an *in vivo* maker for parvalbumin (15–22 days postnatal, 7–11 g, $n = 36$) were used for these studies. The *in vivo* marker in the mouse was enhanced green fluorescent protein (EGFP) that had been inserted in a parvalbumin gene carried on a bacterial artificial chromosome (Meyer *et al.* 2002). Male transgenic mice were bred with female C57BL/6 wild-type mice, and transmission of the transgene was monitored by detecting the EGFP fluorescence in the skin of the hind limbs with ultraviolet illumination (Meyer *et al.* 2002). The transgene was observed in 50% ($n = 181$) of the offspring, in keeping with previous studies on this particular strain of mouse that has multiple integrated copies of the transgene (Meyer *et al.* 2002).

To prepare the brain slices, the animals were anaesthetized with an intraperitoneal injection of Sagatal (sodium pentobarbitone, 80 mg kg^{-1}, Rhône Mérieux Ltd, Harlow, Essex, UK) or with a mixture of ketamine (140 mg kg^{-1}, Fort Dodge Animal Health Ltd, Southampton, UK) and xylazine (14 mg kg^{-1}, Millpledge Pharmaceuticals, UK). When all pedal reflexes were abolished, the rats and mice were perfused intracardially with ice-cold, oxygenated (95% O_2–5% CO_2) artificial cerebrospinal fluid (ACSF) in which the sodium chloride was partially replaced with iso-osmotic sucrose. The composition of this ACSF was (mM): 112.5 sucrose; 63 NaCl; 3 KCl; 1.25 NaH_2PO_4; 24 $NaHCO_3$; 6 $MgSO_4$; 0.5 $CaCl_2$; 10 glucose (305 mosmol l^{-1}). Indomethicin (50 μM) was included in this ACSF to improve preservation of the slice maintained *in vitro* (Hughes *et al.* 2002). Parasagittal slices of the MS/DB (at 350 μm for rat and 300 μm for mouse) were taken within 1 mm of the midline of the brain and cut using a Leica VT1000S vibratome (Leica Microsystems UK, Milton Keynes, UK). The slices were then maintained for at least 1 h at room temperature in a holding chamber, just beneath the surface of ACSF bubbled with carbogen gas (95% O_2–5% CO_2) and containing (mM): 126 NaCl; 3 KCl; 1.25 NaH_2PO_4; 24 $NaHCO_3$; 2 $MgSO_4$; 2 $CaCl_2$; 20 glucose (pH 7.4, 305 mosmol l^{-1}). In the recording bath, the slices were maintained at 29–30°C and submerged in the same oxygenated ACSF solution (flow rate 2 ml min^{-1}). On occasions when cadmium-containing, low-calcium ACSF was used, its composition was (mM): 126 NaCl; 3 KCl; 1.25 NaH_2PO_4; 24 $NaHCO_3$; 6 $MgSO_4$; 0.1 $CaCl_2$; 0.2 $CdCl_2$; 20 glucose.

Whole-cell recording and data acquisition

Whole-cell patch recordings were made with micropipettes (resistances 3–5 MΩ) pulled on a Flaming/Brown electrode puller (Sutter Instruments, Novato, California, USA). The micropipettes contained (mM): 140 potassium gluconate; 5 KCl; 2 $MgCl_2$; 10 Hepes; 2 ATP-Na; 0.4 GTP-Na (pH 7.35, 280 mosmol l^{-1}), based on a formulation by Gloveli *et al.* (2001). Recordings were made in current and in voltage clamp from somata (16–20 μm) visualized by infrared differential interference contrast video-microscopy (Zeiss Axioscope microscope, Hamamatsu CCD camera, Luigs and Neumann Infrapatch set-up, Ratingen, Germany). Images were captured by a frame grabber (Scion Corporation, Alrad Instruments Ltd, Newbury UK) and processed with NIH image (version 1.6). EGFP-positive neurones were recorded from by first selecting the neurone under UV fluorescence (FITC filter) and positioning it at the centre of the eyepiece cross-hairs. The cell was then identified with differential interference contrast optics, and then with infrared-differential interference contrast optics on a predetermined position on the video monitor screen. At the termination of the recording, and before removal of the micropipette, the cell was re-examined under fluorescence optics to confirm that it was EGFP positive.

Recordings were made, in current- and voltage-clamp mode, using Axoclamp 2B and Axopatch 1D amplifiers (Axon Instruments Inc, Union City, CA, USA). The patching process was carried out in current-clamp mode so that neuronal characterization could be performed as soon as the patch seal was broken. Criteria for a good recording were a seal resistance of $\geq$2 GΩ

before acquiring the whole-cell mode, access resistance of <35 MΩ, resting membrane potential of >−45 mV, and spikes that overshot 0 mV. No corrections were made for junction potentials. Recordings were analog-filtered at 1–3 kHz and digitized at 5–10 kHz, i.e. the sampling frequency was set at more than twice that of the filtering frequency, and was highest for recordings required for the measurement of action potential parameters. Recordings were acquired and digitized with an ITC-16 ADC board (Digitimer Ltd, Welwyn Garden City, Hertfordshire, UK) and Axograph software (Axon Instruments), and were further analysed using Axograph (Axon Instruments) software. Extracellular stimulation of fibres was carried out using a tungsten concentric bipolar stimulating electrode (Harvard Apparatus Ltd, Kent, UK) connected to a DS2 isolated stimulator (Digitimer Ltd).

Results are expressed as mean ± S.D. The strength of the association between two variables was assessed using the Pearson product moment correlation test. Statistical significance for comparison between two groups was determined with Student's *t* test or the Mann–Whitney rank sum test. Statistical comparisons for more than two groups were made using either a one-way analysis of variance (ANOVA; Student–Newman–Keuls test) or an ANOVA on ranks (Kruskal–Wallis test). Measures were considered statistically significant if $P < 0.05$. All statistical tests were performed using SigmaStat software (SPSS Inc., California, USA).

Neuronal characterization procedures

To correlate pharmacological responses with neurone cell type, the passive and regenerative membrane properties of each neurone were thoroughly characterized in current-clamp mode before the pharmacological studies were carried out. Membrane properties, single action potential properties and firing patterns were determined as previously described (Jones *et al.* 1999; Morris *et al.* 1999; Morris & Henderson, 2000; Henderson *et al.* 2001). Modifications to the above are described as follows. Spike duration was measured as the period between the start of the rapid phase of the spike upshoot (at slope +45 deg) and the end of the rapid phase of the spike down-shoot (at slope −45 deg). Spike rise time was determined as the period between the start of the rapid phase of the spike upshoot, and the beginning of spike repolarization (at slope 0 deg). It was not possible to make accurate measurements of the parameters of the after-hyperpolarization (AHP), due to the presence of an after-depolarization in most of the recordings of action potentials. The measured, rather than actual, amplitude of the AHP therefore was taken to be the difference in potential between that at the start of the spike (as determined above) and at the most hyperpolarized level of the AHP. To determine the extent of time-dependent inward rectification (depolarizing sag, attributed to an H current, I_H, Griffith, 1988) and rebound (attributed to a low threshold calcium current, I_T, Griffith, 1988), graded hyperpolarizing current steps of 1000 ms were applied from holding potentials of −60 mV to −120 mV. The magnitudes of depolarizing sag and rebound from −80 mV and −90 mV were measured as the potential differences between the peak hyperpolarization and end of the hyperpolarizing step, and between the peak depolarization and the baseline of the ensuing rebound at the end of the hyperpolarizing step, respectively. Neurone firing properties were determined exactly as has been done previously, except that depolarizing current steps of 1000 ms rather than 600 ms were used in the current study. Another additional parameter that was measured was the amplitude of the AHP that follows a train of spikes.

Analysis of pharmacological properties

Drugs were applied by superfusion at a known concentration, and acetylcholine (ACh) by pressure from a micropipette using a Picopump (World Precision Instruments, Stevenage, Hertfordshire, UK), as previously described for the hippocampus (Frazier *et al.* 1998*b*; McQuiston & Madison, 1999). The ACh (3 mM in Hepes/ACSF) was puffed every 30–60 s, at 10 psi for 10–60 ms from patch pipettes of the same dimensions as those used for recording (tip 2−4 μm). The pipette tip was placed beneath the surface of the slice and at a distance of 20–50 μm from the neurone from which the recording was made. Extrusion of the solution during application of the pressure pulse was monitored visually and was indicated by slight movement of the tissue. The composition of the Hepes/ACSF vehicle (also used as a negative control) was as follows (mM): 146 NaCl; 10 Hepes; 2.5 KCl; 2 $CaCl_2$; 2 $MgCl_2$; 5 glucose (pH 7.4; 310 mosmol l^{-1}). The ACh concentration and composition of the vehicle in the puff pipette were the same as those employed by McQuiston & Madison (1999). In some experiments, small hyperpolarizing current pulses (−20 pA, 0.1 Hz) were used to monitor input resistance changes at different holding potentials during application of the ACh.

Immunocytochemistry

To confirm the pharmacological observations made with the whole-cell patch recordings, dual or single immunocytochemical staining for nicotinic receptor subunits, parvalbumin and vesicular ACh transporter (VAChT) was carried out on sections from perfused-fixed tissue. Eleven adult Wistar rats (200–220 g) were deeply anaesthetized with an I.P. injection of ketamine (140 mg kg^{-1}) and xylazine (14 mg kg^{-1}), and perfused intracardially with 500 ml of 4% paraformaldehyde in 0.1 M phosphate

buffer (pH 7.4). The brains were removed and placed in the same fixative for 2–3 h, and then in phosphate buffer overnight at 4°C. Sections were cut at 50 μm in the coronal planes using a Leica VT1000S vibratome (Leica Microsystems UK, Milton Keynes, UK). Optimal results for antigen retrieval were obtained by treatment of the sections with ethanol and methanol solutions prior to carrying out the immunocytochemical staining steps. The sections were washed in 30%, 50%, 70%, 90% and 100% ethanol for 3–4 min each, and then placed in 100% methanol at −20°C for 5 min. The sections were taken through descending solutions of ethanol, and then washed in 0.1% Triton in phosphate-buffered saline (pH 7.4), which was the solution used for all wash solutions and as diluent for the antibody solutions. Unless stated otherwise, all steps were carried out at room temperature and with gentle agitation of the sections. Before incubation in antibody solutions, all sections were incubated for 1 h in 2% bovine serum albumin.

Sections were stained singly for the nicotinic receptor subunits using the antibodies to the α7 nicotinic receptor subunit (1/500 and 1/1000 mouse monoclonal antibody, clone mAb 306, Sigma; 1/300 and 1/600 rabbit polyclonal antibody, Santa Cruz, CA, USA), the α4 nicotinic receptor subunit (1/300 and 1/600 antirabbit polyclonal antibody, Santa Cruz) and the β2 nicotinic receptor subunit (1/300 and 1/600 rabbit polyclonal antibody, Santa Cruz). The sections were incubated overnight at 4°C in primary antibody with 2% bovine serum albumin and 0.4% sodium azide. The primary antibodies were omitted in controls. Following several washes, the sections were incubated for 2 h in 1 : 200 biotinylated horse antimouse or rabbit IgG (Vector Laboratories, Peterborough, UK), as appropriate. The sections were washed several times and incubated for 2 h in 1 : 25 avidin–biotin horseradish peroxidase complex (Vector Laboratories). For added sensitivity (see Henderson *et al.* 1998), the sections that had been incubated in the monoclonal antibody to α7 nicotinic receptor subunit were washed several times, and then incubated in mouse 1/500 mouse peroxidase antiperoxidase (Sigma). After these steps the sections were washed several times in 0.05 M Tris buffer at pH 8.0 and then incubated for 5–10 min in 0.006% H_2O_2, 0.014% diaminobenzidine (DAB) and 0.6% nickel ammonium sulphate in 0.05 M Tris buffer at pH 8.0 (Wouterlood *et al.* 1987). The sections were washed in 0.05 M Tris buffer, and then several times in 0.1 M phosphate buffer. The sections were mounted on slides under coverslips in solvent-based mounting medium in the conventional manner.

To determine in which cell type in the MS/DB the nicotinic subunits were located, the rabbit polyclonal antibodies to the α4 or the β2 nicotinic receptor subunit were made up in either 1 : 4000 goat anti VAChT (Chemicon International Inc., Harrow, UK) or in 1 : 6000 mouse antiparvalbumin (PARV-19 clone; Sigma). In control sections one or both antibodies were omitted from the steps. The sections were incubated overnight at 4°C in the primary antibody solutions, washed several times and incubated for 2 h in 1 : 200 Texas Red donkey antirabbit IgG (Stratech Scientific Ltd, Soham, UK). The sections were then washed several times and some were taken out at this stage for controls. The remainder of the sections were incubated for 2 h in either 1 : 500 biotinylated horse antimouse IgG (Vector Laboratories) or 1 : 500 biotinylated horse antigoat IgG (which ever was appropriate), washed several times and incubated for 2 h in 1 : 500 Alexa–Fluor 488–streptavidin (Molecular Probes Europe BV, Leiden, Netherlands). The sections were then washed several times and mounted on slides. Just before the sections were about to dry out, they were embedded under coverslips in glycerol and the coverslips sealed with nail varnish. The sections were viewed with a Zeiss LSM 510 Meta confocal microscope (Zeiss, Welwyn Garden City, Herts., UK).

Materials

All standard reagents, except where indicated, were obtained either from Sigma (Poole, Dorset, UK) or VWR International (Lutterworth, Leicesterhire, UK). Bicuculline methochloride, 2,3,-dioxo-6-nitro-1,2,3,4,-tetrahydrobenzo[f]quinoxaline-7-sulphonamide disodium (NBQX), D-(−)-2-amino-5-phosphonopentanoic acid (D-AP5), MDL72222, suramin and tetrodotoxin citrate (TTX) were purchased from Tocris Cookson (Avonmouth, UK). Acetylcholine chloride, atropine sulphate, mecamylamine, methyllycaconitine, α-bungarotoxin, dihydro-β-erythroidine (DHβE) and physostigmine hemisulphate, were obtained from Sigma. Stock solutions of the pharmacological agents were made up at ×1000 their working concentration in H_2O, except for NBQX and MDL72222 which were made up in DMSO, and stored as aliquots at −45°C.

Results

Characterization of neurones

Recordings were made from the parts of the MS/DB shown previously to be rich in parvalbumin-containing neurones and cholinergic neurones (Kiss *et al.* 1990). The neurones in rat and mouse MS/DB were subdivided into slow firing (putative cholinergic) neurones and into burst firing and fast firing (putative GABAergic) neurones, on the basis of previous criteria. Slow firing neurones (rat: $n = 34$) were distinguished from the other cell types by their lack of depolarizing sag and rebound (Gorelova & Reiner, 1996; Sotty *et al.* 2003). Burst firing cells (rat: $n = 15$; mouse: $n = 5$) were distinguished on the basis of a voltage-dependent

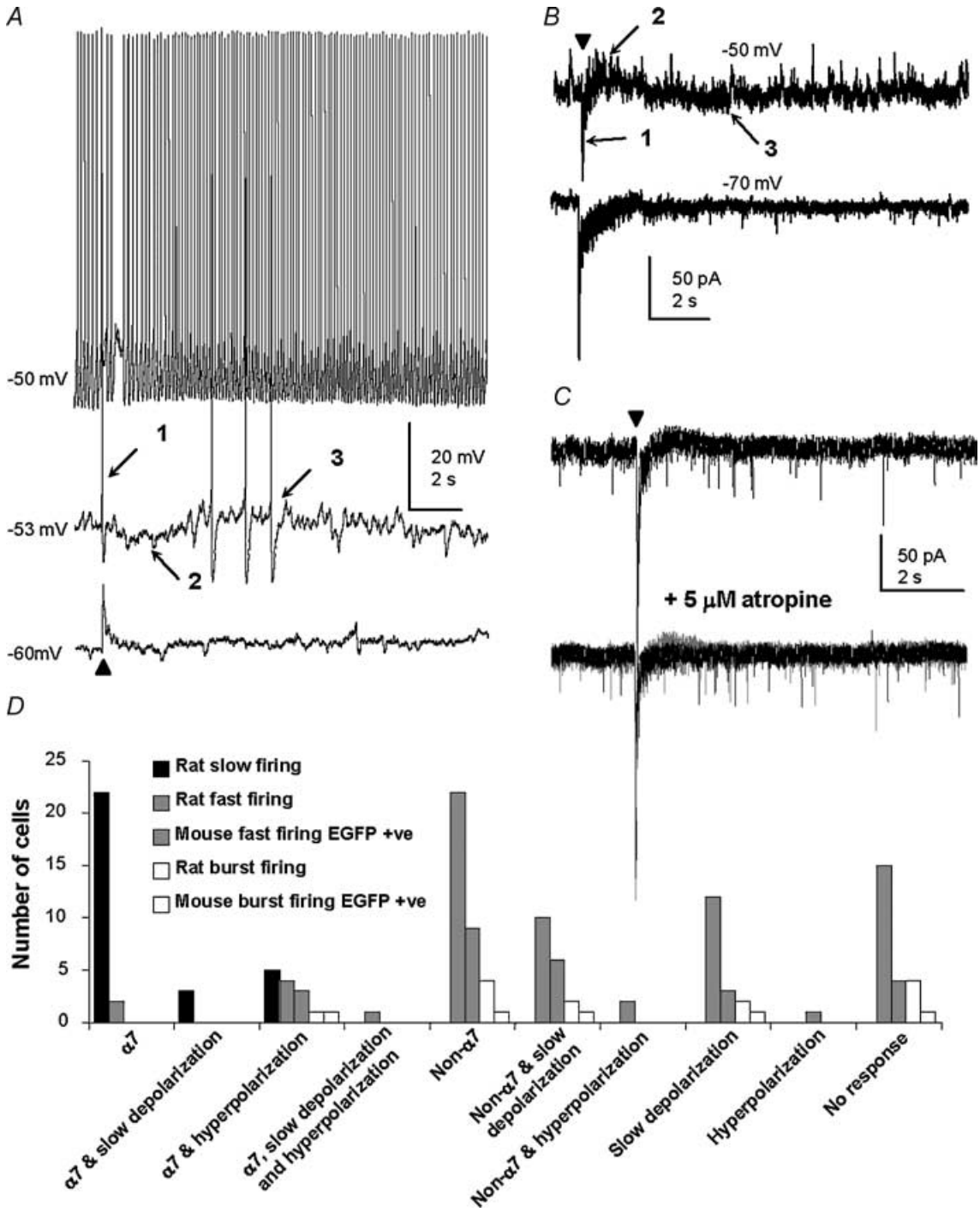

Figure 1. Examples of different types of responses to puffed ACh
A, a fast firing cell recorded at –50, –53 and –60 mV, showing changes in amplitudes of the fast depolarization (1), fast hyperpolarization (2) and slow depolarization (3) with variation in the membrane potential. The filled triangle in this figure and in all subsequent figures, indicates when the brief (10–60 ms) application of ACh was made. *B*, responses of the same fast firing cell as in *A* are shown, this time as recordings in voltage-clamp mode at –50 and at –70 mV. The equivalents to the fast depolarization (1) and slow depolarization (3) are visible as inward currents, while the equivalent to the fast hyperpolarization (2) is visible as an outward current. *C*, a fast firing cell, voltage clamped at –70 mV, showing block of the outward current response to ACh by 5 μM atropine (the previous trace, shown in grey, is superimposed). *D*, bar chart showing the different types of responses of characterized MS/DB neurones in rat and mouse to puffed ACh. The symbols α7 and non-α7 refer to responses attributed to the presence of α7*-type nicotinic and non-α7*-type nicotinic receptors, respectively, as determined from pharmacological investigation and kinetics of the responses. EGFP-positive neurones are those that correspond to parvalbumin-containing cells in the mouse.

burst response following depolarization from −75 mV (Griffith & Matthews, 1986; Griffith, 1988). The remaining neurones (rat: $n = 89$; mouse: $n = 32$) were classed as fast firing neurones (Griffith & Matthews, 1986; Griffith, 1988). The three neurone types were also distinguished by statistical differences of measured features such as size and various electrophysiological parameters, in keeping with previous studies (Griffith & Matthews, 1986; Griffith, 1988; Gorelova & Reiner, 1996; Morris *et al.* 1999; Morris & Henderson, 2000; Henderson *et al.* 2001).

Responses of neurones to puffed ACh

Responses of neurones to ACh in rat MS/DB were tested in the three major cell types which are referred to below as: S, slow firing; F, fast firing; and B, burst firing. Positive responses to puffed 3 mM ACh were found in all types of cells (S = 30/30 F = 53/68, B = 9/13) and these cells were randomly distributed in the MS/DB. Application of the vehicle alone to an ACh-responsive cell did not result in a positive response. The responses to ACh were in the form of fast depolarizations (duration: 0.3–4.8 s, $n = 78$), fast hyperpolarizations (duration: 1.2–4.5 s, $n = 13$) and slow depolarizations (duration: 7–30 s, $n = 30$) that occurred singly or in various combinations.

The slow depolarization response to puffed ACh (e.g. labelled '3′ in Fig. 1*A*) was seen in all cell types (S = 3, F = 23, B = 4), and was assumed to be of muscarinic receptor origin because (1) it was slow in onset and prolonged, (2) in voltage-clamp mode it appeared as a slow inward current (e.g. labelled '3' in Fig. 1*B*), (3) its amplitude became larger with increased depolarization of the membrane potential (e.g. Fig. 1*A* and *B*), and (4) it was blocked with 5 μM of the muscarinic receptor antagonist

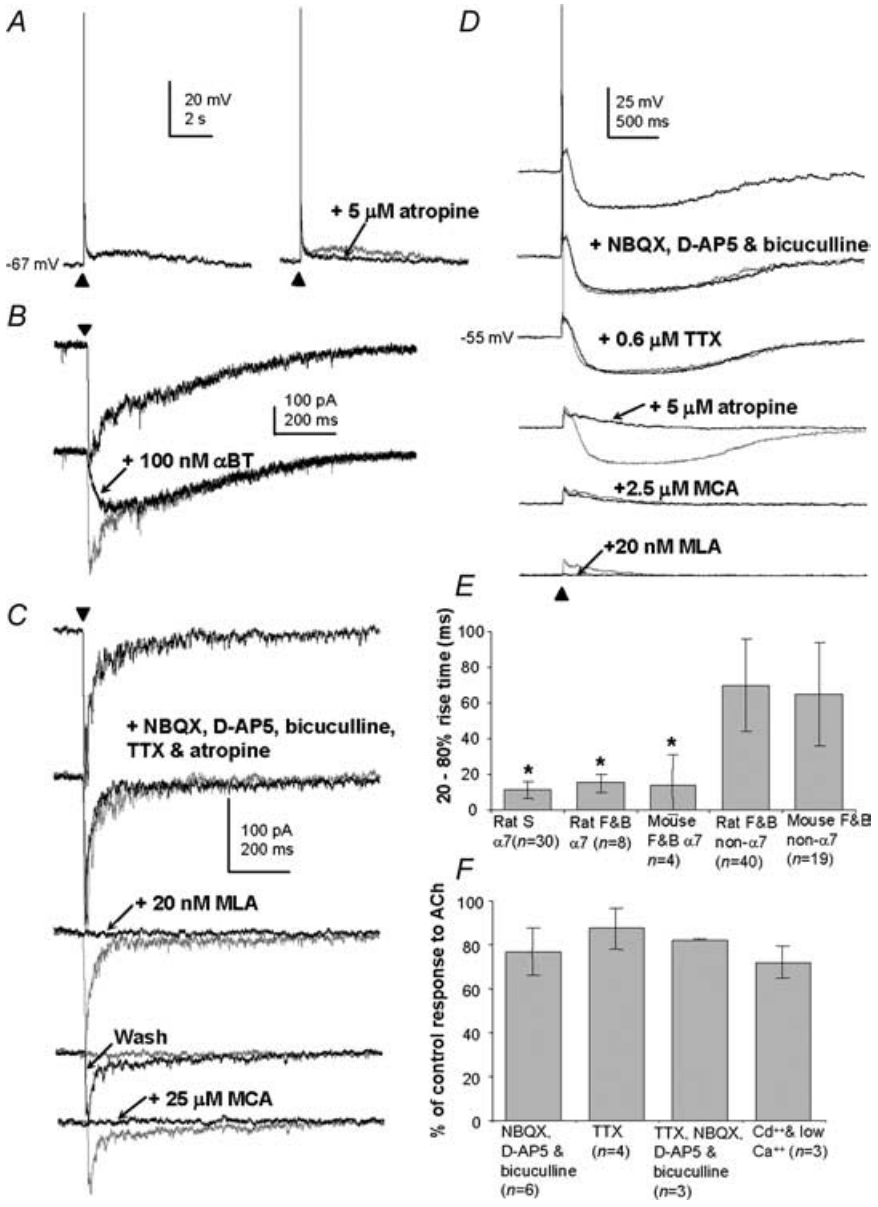

Figure 2. Examples of α7* nicotinic receptor-type responses of MS/DB cholinergic and GABAergic neurones to puffed ACh
A, a slow firing cell showing a fast depolarization response that produced a single action potential plus a slow depolarization that was blocked by 5 μM atropine. *B*, a voltage-clamp recording, at –60 mV, from a slow firing cell responding to ACh, showing partial block of the inward current response by 100 nM α-bungatotoxin. The remaining response had a slower rise time than the original. *C*, a voltage-clamp recording, at –70 mV, from a slow firing cell responding to ACh, showing the effects of the bath application of 20 μM NBQX, 50 μM D-AP5 and 20 μM bicuculline, followed by 20 nM methyllycaconitine (MLA) with recovery, then 25 μM mecamylamine (MCA). *D*, a fast firing neurone responding to ACh, showing the effects of application of 20 μM NBQX, 50 μM D-AP5 and 20 μM bicuculline, followed by 0.6 μM TTX, 5 μM atropine, 2.5 μM mecamylamine (MCA) and then 20 nM methyllycaconitine (MLA). *E*, bar chart showing the 20–80% rise times of characterized ACh responses of identified cells. Abbreviations: α7 and non-α7 are responses attributed to the presence of α7*-type nicotinic and non-α7*-type nicotinic receptors, respectively; S, slow firing neurone type; F, fast firing neurone type; B, burst firing neurone type. The symbol * indicates that there was a statistically significant difference between the rise times of α7*-type nicotinic and non-α7*-type nicotinic receptor responses. *F*, bar chart showing relative changes in the amplitude the α7* nicotinic receptor subtype responses in slow firing neurones after application of various agents. Error bars indicate S.D.

atropine (S = 3, F = 6, B = 2). The fast hyperpolarization elicited in response to puffed ACh (e.g. labelled '2' in Fig. 1*A*) was seen in all cell types (S = 5, F = 7, B = 1) and was also likely to be of muscarinic receptor origin because (1) in voltage-clamp mode it appeared as an outward current (e.g. labelled '2' in Fig. 1*B*), (2) it became larger with increased depolarization of the membrane potential (e.g. Fig. 1*A* and *B*), and (3) it was blocked with 5 μM atropine (S = 3, F = 4, e.g. Fig. 1*C*) but not with the $GABA_A$ receptor antagonist bicuculline (F = 2).

The fast depolarization in response to ACh (e.g. labelled '1' in Fig. 1*A*) was seen in all cell types (S = 30; F = 41; B = 7) and appeared to be of nicotinic receptor origin because (1) it was rapid in onset and was associated with a decrease in input resistance (not illustrated), (2) in voltage-clamp mode it appeared as an inward current (e.g. Fig. 1*B* and *C*), (3) its amplitude decreased with increased membrane depolarization (Fig. 1*B*), (4) it was resistant to 5 μM atropine (S = 15; F = 17, B = 2, e.g. Figure 1*C*), and (5) it was completely and reversibly blocked with a high concentration (25 μM) of the nicotinic receptor antagonist mecamylamine (S = 3, F = 10; B = 1). The properties of the nicotinic receptor responses in the individual cell types will now be described.

Nicotinic receptor responses of slow firing (putative cholinergic) neurones. Slow firing cells (30/30) possessed a fast depolarizing response to puffed ACh with a duration of 1.5 ± 0.8 s, and which at -50 to -60 mV elicited a single action potential ($n = 30/30$, e.g. Fig. 2*A*). At holding potentials of -65 to -75 mV, there was a depolarization but no action potential. The size of the response was 20 ± 8 mV ($n = 26$) and had a 20–80% rise time of 11 ± 5 ms ($n = 30$, Fig. 2*E*, first column). In voltage-clamp mode (at -65 mV to -75 mV), the response was in the form of an inward current with a peak ranging from 47 to 573 pA ($n = 11$). The response to ACh was blocked completely and reversibly with 25 μM mecamylamine (S = 3). It was also blocked completely or partially (to 7–57% of peak response) with 10–20 nM of the specific and reversible $\alpha7^*$ nicotinic receptor subtype antagonist methyllycaconitine ($n = 12$) or with 100 nM of the specific and irreversible $\alpha7^*$ nicotinic receptor subtype antagonist α-bungarotoxin ($n = 3$). In cases where the block in response was partial (e.g. Fig. 2*B*), the remaining response had a significantly longer 20–80% rise time than the initial response (from 8.5 ± 5.7 to 73.4 ± 92.5 ms, $P < 0.05$, Wilcoxon signed rank test, $n = 7$). This remaining response was blocked by 2.5 μM mecamylamine ($n = 3$; not illustrated). These results suggest that the response of the MS/DB cholinergic neurone to puffed ACh is made up either entirely of an $\alpha7^*$ nicotinic receptor subtype component, or of a combination of an $\alpha7^*$ nicotinic receptor and a non-$\alpha7^*$ nicotinic receptor subtype component.

To determine whether the responses of the slow firing neurones to puffed ACh were presynaptic or somatic–dendritic in origin, ACh was puffed in the presence of ACSF containing either ionotropic glutamatergic and GABAergic receptor antagonists 20 μM NBQX, 50 μM D-AP5 and 20 μM bicuculline, or 0.6 μM TTX, or a combination of TTX, NBQX, D-AP5 and bicuculline, or 200 μM cadmium and 0.1 mM (i.e. low) calcium. The investigations were carried out in current- and in voltage-clamp mode at -60 to 70 mV. The efficacy of each blocker was assessed by looking for the disappearance of stimulus-evoked synaptic potentials in the case of ionotropic glutamate and GABA receptor antagonists, or cadmium and low calcium, and by the disappearance of action potentials in the case of TTX in current-clamp mode and of large postsynaptic currents when TTX was applied in voltage-clamp mode. The changes to the ACh responses were assessed by measuring the peak average of 4–8 successive responses, and by examination of changes in the waveform of the responses seen after superposition of the traces. For the slow firing cells, there was a drop in peak response to puffed ACh (compared to control) to $77 \pm 11\%$ ($n = 6$) in the presence of NBQX, D-AP5 and bicuculline, to $87 \pm 9\%$ ($n = 4$) in the presence of TTX, to $82 \pm 1\%$ ($n = 3$) in the presence of TTX, NBQX, D-AP5 and bicuculline and to $72 \pm 7\%$ ($n = 3$) in the presence of cadmium and low calcium (e.g. Fig. 2*C*, and see Fig. 2*F*). In some cases there was in addition, a steeper decay of the response afterwards ($n = 6/16$). The responses remaining after these treatments were blocked either completely or partially by 10–20 nM methyllycaconitine or by 100 nM α-bungarotoxin ($n = 10$, e.g. Fig. 2*C*). In cases where the block with these agents was partial ($n = 4$), superposition of the traces indicated that there was a disappearance of a fast component to the response indicated by a less steep rise time in the response. These results suggest the presence of somato-dendritic $\alpha7^*$ and non-$\alpha7^*$ nicotinic receptor subtypes on putative cholinergic neurones of the MS/DB.

Nicotinic receptor responses of fast and burst firing (putative GABAergic) neurones in rat and mouse. Responses of neurones to ACh were studied in MS/DB slices from rat and transgenic mouse. In the transgenic mice the distribution of the EGFP-positive cells in the brain was as previously described (Meyer *et al.* 2002), and followed the pattern seen for parvalbumin-containing neurones in the CNS (Celio, 1990). No EGFP-positive neurones were observed in MS/DB slices from wild-type littermates. EGFP-positive cells were electrophysiologically characterized using the same criteria as that for rat cells, and $n = 32$ were of the fast firing type and $n = 5$ of the burst firing type. Within the fast firing and burst firing groups from both species, no distinctive property of the response to

ACh, i.e. whether it was null response, slow depolarization alone, or a specific type of fast depolarization (see below), could be associated with any statistical difference between the measured electrophysiological parameters of the cells (data not shown), or with the presence of parvalbumin (Fig. 1*D*). For simplicity therefore, the fast firing and burst firing cells from both species are collectively referred to in the next sections as 'GABAergic' cells.

Two versions of fast depolarization were observed in the GABAergic cells, on the basis of whether the ACh puff elicited a single action potential at –50 to –60 mV ($n = 12$, e.g. Fig. 2*D*), or two or more action potentials on a depolarizing wave ($n = 59$). The 20–80% rise time for the former response was 15 ± 5 ms for rat ($n = 8$) and 14 ± 17 ms for mouse ($n = 4$), and these values were not significantly different from that for the rat slow firing cells ($P > 0.05$, Kruskal–Wallis ANOVA on ranks test with Dunn's comparison procedure; Fig. 2*E*). Often, the first type of fast depolarizing response was accompanied by a prominent fast hyperpolarization ($n = 11/12$, e.g. Fig. 3*D*), that was occasionally observed also in slow firing neurones ($n = 5/30$, not illustrated). This type of fast depolarization was fully and reversibly blocked with 20 nM methyllycaconitine ($n = 4$, e.g. Fig. 2*D*), as it was in the cholinergic cells.

In the GABAergic cells that had fast depolarizing responses to puffed ACh in the form of two or more spikes ($n = 59$, e.g. Fig. 3*A*), the response was of a duration of 2.3 ± 0.9 s for rat ($n = 40$) and 2.1 ± 1.1 s for mouse ($n = 19$). In current-clamp mode at −65 mV to −75 mV, the peak response was 22 ± 12 mV for rat ($n = 33$), and 19 ± 9 mV for mouse ($n = 16$). In voltage-clamp mode at −65 to −75 mV, the peak response ranged from 40 to 857 pA for rat cells ($n = 13$). The 20–80% rise time of the response was 70 ± 26 ms for rat cells ($n = 36$), and 65 ± 26 ms for mouse cells ($n = 17$), and was significantly greater than those for the slow firing, fast firing and burst firing cells that had $\alpha 7^*$ nicotinic receptor-type responses ($P < 0.05$, Kruskal–Wallis ANOVA on ranks test; Fig. 2*E*). The responses in the former were completely and reversibly blocked by 25 μM mecamylamine ($n = 12$, e.g. Fig. 3*B*), but only slightly or not at all with 10–20 nM methyllycaconitine (to 87 ± 14% of control, $n = 14$, e.g. Fig. 3*C* and *D*) and with no change in the rise time of the response when the traces were normalized and superimposed. The responses were either profoundly reduced by 0.1 μM of the nicotinic receptor antagonist dihydro-β-erythroidine (DHβE; to 17 ± 15% of control, $n = 9$, e.g. Fig. 3*C*), or were relatively insensitive to 0.1 μM DHβE (reduced to 78 ± 15% of control, $n = 8$), but sensitive to 2.5 μM mecamylamine (responses reduced to to 9 ± 10% of control, $n = 5$, e.g. Fig. 3*D*).

No significant change in the size or shape of the response to ACh in these GABAergic neurones was evident in the presence of 20 μM NBQX, 50 μM D-AP5 and 20 μM bicuculline ($n = 4$, e.g. Fig. 4*A* and see Fig. 4*C*). The responses to TTX were more variable, and the average drop in peak response to puffed ACh (compared to control) was to 78 ± 21% in the presence of 0.6 μM TTX ($n = 9$, e.g. Fig. 4*B* and see Fig. 4*C*), and to 36 ± 7% in the presence of TTX, NBQX, D-AP5 and bicuculline, with recovery ($n = 4$; Fig. 4*C*). It was rarely possible to properly assess the responses of the GABAergic cells to ACh in the presence of 200 μM cadmium and 0.1 mM calcium, because this often caused these cells to fire uncontrollably. In cases where such recordings were successful, no reduction in size of the fast depolarizing response to ACh was observed ($n = 3$, e.g. Fig. 4*B*, and see Fig. 4*C*). The responses remaining after these treatments were blocked completely with 25 μM mecamylamine ($n = 10$, e.g. Fig. 4*A* and *B*). These results suggest that a proportion of GABAergic cells in the MS/DB possess somato-dendritic nicotinic receptors predominantly of the non-$\alpha 7^*$ nicotinic receptor subtype, and which may be composed of a variety of nicotinic receptor subunits.

Investigation of cholinergic synaptic responses

Recordings were performed in the current-clamp mode, and the neurones selected for study were those shown to have fast depolarizing responses to puffed ACh. The stimulating electrode was placed in sites known to be rich in acetylcholinesterase-positive fibres (Paxinos & Watson, 1986). Either a single stimulus (up to 80 V, 0.1 ms long), or a train of six pulses at 200 Hz was applied every 30 s, and five traces were averaged for each episode. Alternatively, the recording was made in 'chart' mode to assess the time course of effects of receptor antagonists. Once suitable evoked postsynaptic potentials (PSPs) were recorded, the recordings were repeated in the presence of ionotropic receptor antagonists that included 20 μM bicuculline, 50 μM D-AP5, 20 μM NBQX, 100 μM suramin (ATP receptor antagonist) and 0.5 μM MDL 72222 (5-HT_3 receptor antagonist). In some cases 5 μM physostigmine hemisulphate was included ($n = 6$). The responses were recorded at −85 mV to −90 mV, to counteract the effects of metabotropic receptor responses. In all the experiments carried out, no residual evoked response remained that was reversibly blocked with 25 μM mecamylamine in cells identified as either cholinergic ($n = 5$) or GABAergic ($n = 26$). Similarly, no residual spontaneous PSPs remained in the presence of the non-nicotinic ionotropic receptor antagonists in the recordings from these cells. It was concluded therefore that somato-dendritic nicotinic receptors in the MS/DB are not primarily located at cholinergic synapses and do not mediate fast cholinergic transmission there.

Immunocytochemistry

Immunocytochemical staining for the nicotinic receptor subunits $\alpha 4$, $\beta 2$ and $\alpha 7$ was carried out using DAB and

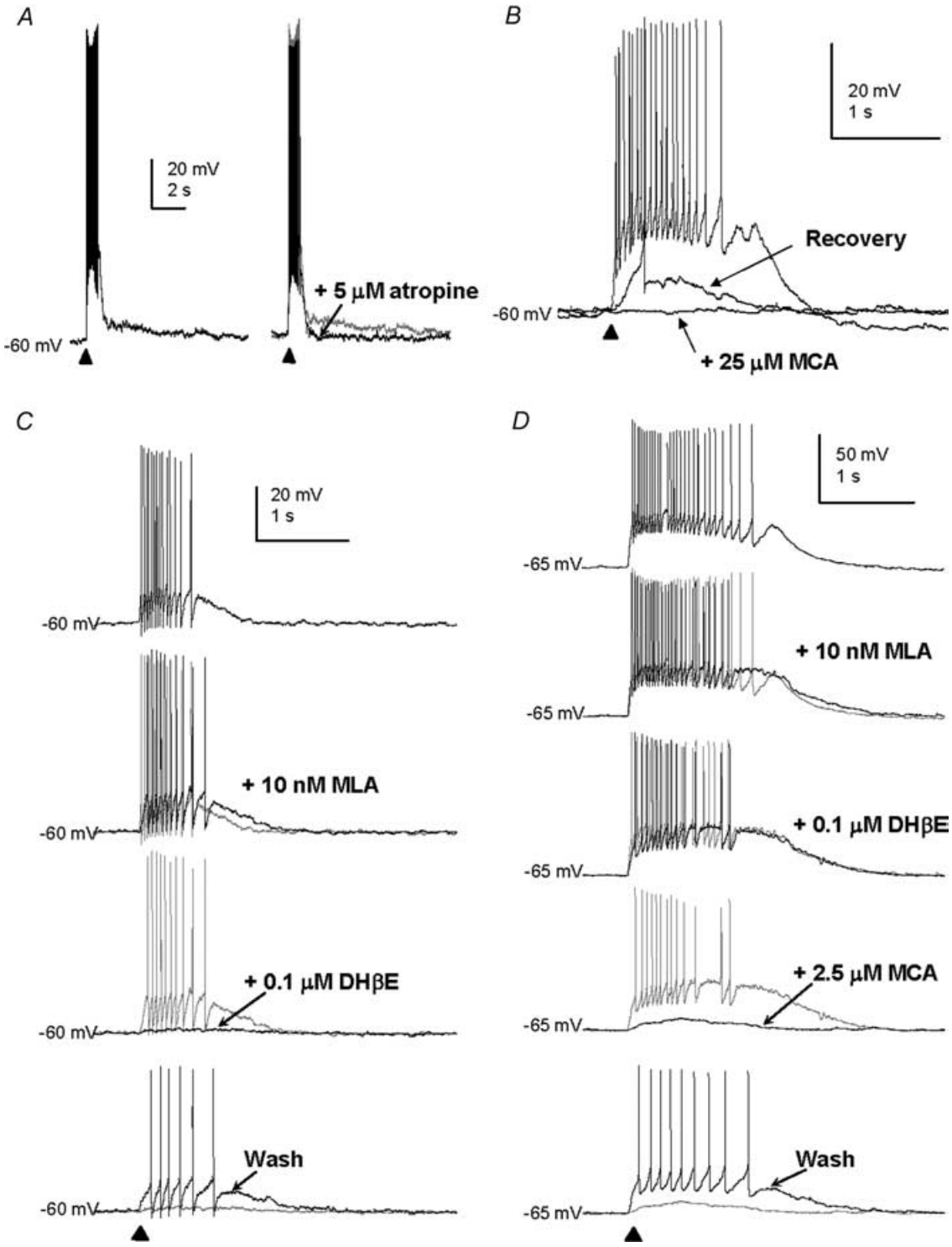

Figure 3. Examples of non-α7* nicotinic receptor-type responses of MS/DB GABAergic neurones to puffed ACh

A, a fast firing neurone showing a fast depolarization response that produced a burst of spikes, followed by a slow depolarization that was blocked with 5 μM atropine. *B*, a fast firing cell, showing block of the fast depolarization response to ACh by 25 μM mecamylamine (MCA), with recovery after washout of the antagonist. *C*, a fast firing neurone with an ACh response, showing the effects of application of 10 nM methyllycaconitine (MLA), followed by 0.1 μM DHβE, then recovery of the response after washout of the antagonist. *D*, a fast firing neurone with an ACh response, showing the effects of the application of 10 nM methyllycaconitine (MLA) followed by 0.1 μM DHβE then 2.5 μM mecamylamine, with recovery of the response after washout of the antagonist.

immunofluorescence methods. No specific staining was observed in the controls. The specificity of the immunocytochemical labelling was also assessed by examination of the staining for these receptor subunits in areas that have been well characterized in other publications (see below). With the monoclonal antibody to the α7 nicotinic receptor subunit (but not the polyclonal antibody), prominent staining of dendrites and somata of interneurones, but not of pyramidal neurones, was observed in the hippocampal formation (not illustrated), as expected from

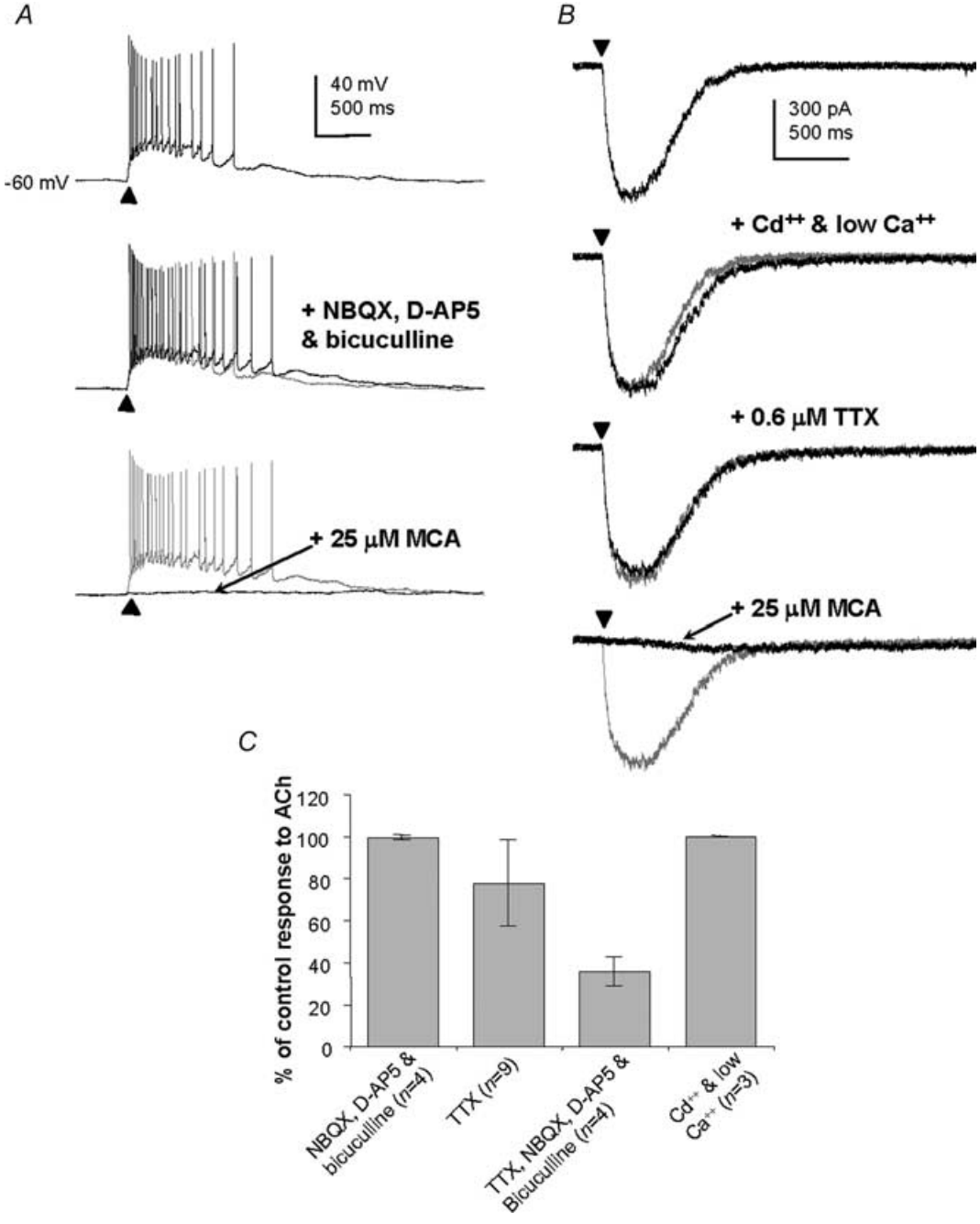

Figure 4. Effects of various agents on non-α7* nicotinic receptor-type responses of MS/DB GABAergic neurones to puffed ACh

A, a voltage-clamp recording, at –70 mV, from a fast firing neurone showing the effects of application of cadmium and low calcium, followed by 0.6 μM TTX, then 25 μM mecamylamine (MCA). *B*, a fast firing neurone with an ACh response, showing the effects of application of 20 μM NBQX, 50 μM D-AP5 and 20 μM bicuculline, followed by 25 μM mecamylamine (MCA). *C*, bar chart showing relative changes in the amplitudes of the non-α7* nicotinic receptor-type responses after application of non-nicotinic ionotropic receptor antagonists, TTX and cadmium and low calcium. Error bars indicate S.D.

electrophysiology (Frazier *et al.* 1998*b*). Punctate staining for the α7 nicotinic receptor subunit was also prominent in many parts of the brain, e.g. the ventral striatum, presumably reflecting the presynaptic location of this receptor subunit (Wonnacott *et al.* 2000). There was staining for the α7 nicotinic receptor subunit in somata in the MS/DB in the DAB preparations (Fig. 5*A*), but this was not detectable above background with immunofluorescence, so double-label analysis was not successful. With the polyclonal antibody to the α4 nicotinic receptor subunit, staining of neuronal cell bodies was observed in select areas of the brain, and was especially prominent in the substantia nigra zona compacta, as reported previously (Sorenson *et al.* 1998; Arroyo-Jiménez *et al.* 1999). Prominent staining of cell bodies for the α4 nicotinic receptor subunit was observed in the MS/DB with the DAB method (Fig. 5*B*). Double immunofluorescence indicated that labelling for the α4 nicotinic receptor subunit was localized in both parvalbumin-positive and parvalbumin-negative somata in the preparations double labelled for parvalbumin and the α4 receptor subunit. It was absent, however, from the majority of VAChT-positive neurones in the preparations double labelled for VAChT and the α4 receptor subunit (Fig. 5*D–G* and Fig. 7*A*,*B*). Using antibodies to the β2 nicotinic receptor subunit, there was labelling of cell bodies also in the substantia nigra as reported previously (Sorenson *et al.* 1998; Arroyo-Jiménez *et al.* 1999). Punctate staining of the neuropil, presumably reflecting the presynaptic location of the β2 nicotinic receptor subunit, was prominent in the neostriatum, as reported previously (Jones *et al.* 2001). Labelling for the β2 nicotinic receptor subunit was intense in MS/DB somata when the DAB immunocytochemistry method was used (Fig. 5*C*). Double immunfluorescence indicated that the staining for the β2 nicotinic receptor subunit was present in parvalbumin-positive and parvalbumin-negative cells in the preparations double labelled for parvalbumin and the β2 receptor subunit, and in VAChT-positive and VAChT-negative cells in preparations double labelled for VAChT and the β2 receptor subunit (Fig. 6). In summary, the distribution of the labelling for the β2 receptor subunit was similar to that of the α4 receptor subunit in parvalbumin-stained material (Figs 7*A* and *C*) but was different from that of the α4 receptor subunit in VAChT-stained material (Figs 7*B* and *D*).

Discussion

Somato-dendritic nicotinic receptor responses in the MS/DB

In this study we showed that local application of ACh causes fast depolarization of GABAergic and cholinergic neurones in the MS/DB. These responses were inhibited with nicotinic receptor antagonists and they showed variable sensitivity to TTX, but were not completely blocked by this agent or by cadmium, or by antagonists of other ionotropic receptors. These results suggest that there are somato-dendritic nicotinic receptors present on cholinergic and GABAergic neurones of the MS/DB. Nicotinic receptor responses have previously been recorded in the MS/DB *in vivo* (Lamour *et al.* 1984) and *in vitro* (Segal, 1986; Wu *et al.* 2003a), and also in the nucleus basalis *in vitro* (Harata *et al.* 1991). According to Wu *et al.* (2003*a*), however, all the nicotinic receptor responses in the MS/DB slice were attributed to presynaptically located receptors, because TTX in their experiments totally blocked the effect of bath application of nicotine on GABAergic neurones. Nevertheless, it was shown previously that ACh applied as microdrops to MS/DB neurones causes potent depolarization in the presence of TTX (Segal, 1986). These discrepancies could be due to the nature of the agonist and the way it was applied to the MS/DB slice in the different experiments. In hippocampal interneurones, the nicotinic receptor responses were unaltered by TTX and cadmium (Frazier *et al.* 1998*b*; McQuiston & Madison, 1999), whereas in the substantia nigra some of the nicotinic receptor responses were partially affected by TTX (Sorenson *et al.* 1998), as we found in the MS/DB. A possible explanation for this variability in response to ACh in the presence of TTX is that in some cases the puff causes intense depolarization of dendrites, and therefore activation of dendritic voltage-sensitive sodium channels which are blocked by TTX. The final interpretation of the results in the MS/DB is that nicotinic receptors in the MS/DB are located both presynaptically and somato-dendritically.

In our studies, the pharmacological dissection of the responses of MS/DB neurones to puffed ACh revealed the presence of α7* nicotinic receptor types in all cholinergic neurones and in 10% of GABAergic neurones, and non-α7*-type nicotinic receptors subtypes in 50% of GABAergic neurones. These distinctions were also evident from the kinetics of the responses, as α7* nicotinic receptor subtypes have faster activation kinetics than non-α7* nicotinic receptor subtypes (Pereira *et al.* 2002). It cannot be ruled out, however, that the GABAergic neurone with the α7* nicotinic receptor responses represents a cholinergic subtype, because a neurone type that expresses both cholinergic and GABAergic enzymes has been recently described in the MS/DB using single-cell RT-PCR (Sotty *et al.* 2003).

In the GABAergic neurones in the MS/DB, there was evidence for the presence of non-α7* nicotinic receptor subtypes, i.e. those that were sensitive to low concentrations of DHβE and others that were more sensitive to low concentrations of mecamylamine. These two non-α7* nicotinic receptor subtypes, along with the

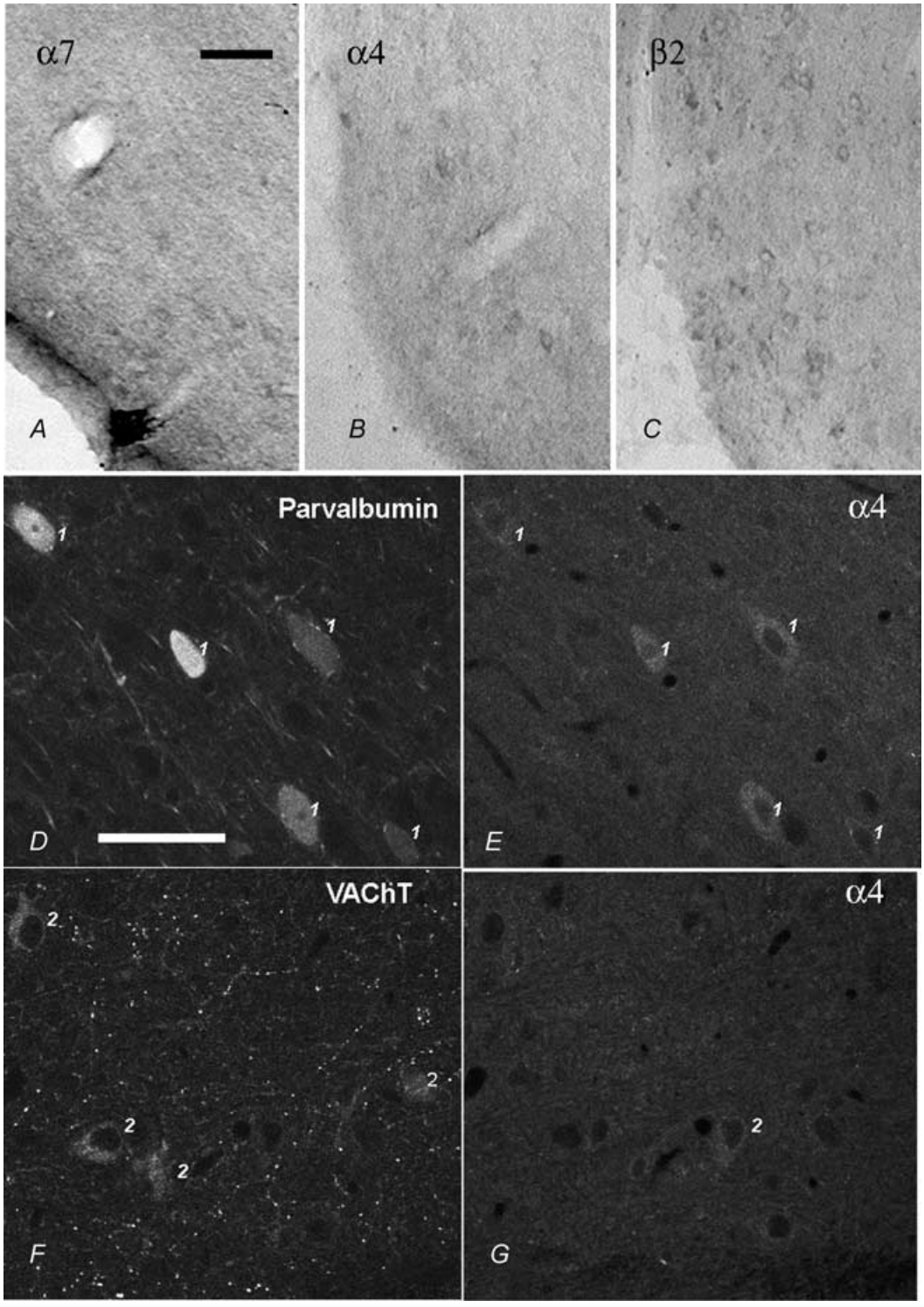

Figure 5. Immunocytochemical staining for the α7, α4 and β2 nicotinic receptor subunits in the MS/DB
A–C, staining for receptor subunit immunoreactivity with the DAB method showing the distribution of α7, α4 and β2 nicotinic receptor subunits, respectively, in somata as viewed with bright field optics. Calibration bar = 100 μM. *D–G*, staining using a dual immunofluorescence method for parvalbumin (*D*, FITC filter) and the α4 nicotinic receptor subunit (*E*, rhodamine filter), or for VAChT (*F*, FITC filter) and the α4 nicotinic receptor subunit (*G*, rhodamine filter), as viewed by confocal microscopy. Double-labelled neurones are indicated by a '1' and single labelled neurones by a '2'. Calibration bar = 50 μm.

α7* nicotinic receptor subtype, seem to correspond to the three types of nicotinic receptor current recorded in hippocampal interneurones in response to ACh (Albuquerque *et al.* 1997; Jones & Yakel, 1997; Frazier *et al.* 1998*b*; McQuiston & Madison, 1999). Type I current (attributed to α7* nicotinic receptor subtypes) is blocked by 10 nM methyllycaconitine, but not by 0.1 μM DHβE or 1 μM mecamylamine. Type II current (attributed

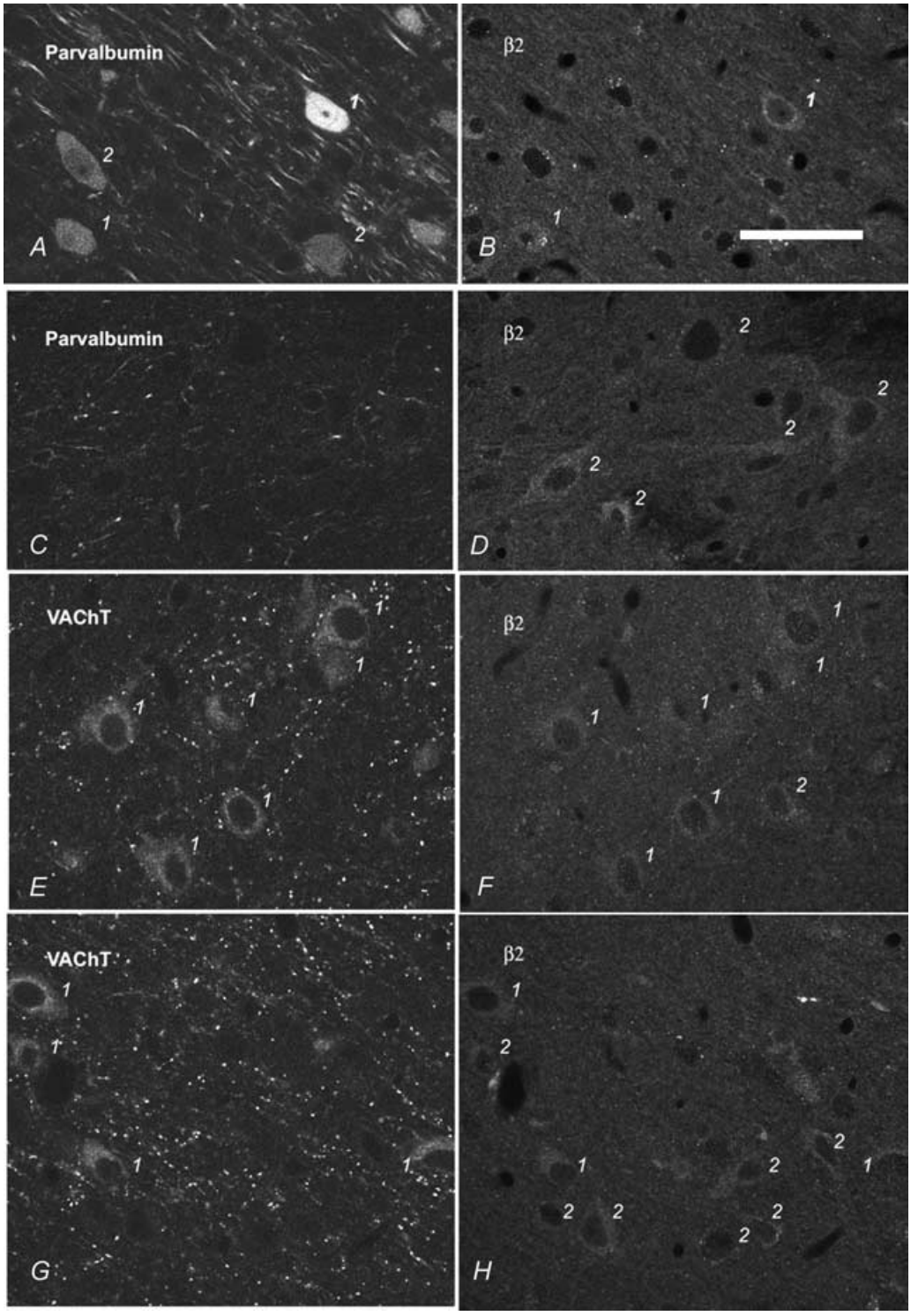

Figure 6. Staining using a dual immunofluorescence method for parvalbumin (*A* and *C*, FITC filter) and the β2 nicotinic receptor subunit (*B* and *D*, rhodamine filter), or for VAChT (*E* and *G*, FITC filter) and the β2 nicotinic receptor subunit (*F* and *H*, rhodamine filter) and as viewed by confocal microscopy
Double-labelled neurones are indicated by a '1' and single-labelled neurones by a '2'. Calibration bar = 50 μm.

to $\alpha4/\beta2^*$ nicotinic receptor subtypes) is blocked 0.1 μM DHβE but not by 10 nM methyllycaconitine or 1 μM mecamylamine. Type III current (attributed to $\alpha3/\beta4^*$ nicotinic receptor subtypes) is blocked by 1 μM mecamylamine but not by 10 nM methyllycaconitine or by 0.1 μM DHβE. The MS/DB neurones therefore seem to possess a complement of nicotinic receptor responses not unlike that found among interneurones in the hippocampus.

The nicotinic receptor subunits that are found in the CNS as a whole include subunits $\alpha2$–7 and $\beta2$–4, but the most abundant are subunits $\alpha4$, $\alpha7$ and $\beta2$ (Wada *et al.* 1989; Clementi *et al.* 2000), which we detected in neurones in the MS/DB using immunocytochemistry. The distribution of the labelling for the $\alpha4$ and $\beta2$ nicotinic receptor subunits in tissue double labelled for parvalbumin or VAChT suggested that the $\beta2$ receptor subunit is colocalized with the $\alpha4$ receptor subunit in parvalbumin-positive cells, but with another unknown α nicotinic receptor subunit in the cholinergic cells. We found cellular staining for $\alpha7$ nicotinic receptor subunit immunoreactivity in cell bodies in the MS/DB, as described by previous workers (Deltoro *et al.* 1994), but were not able to perform double labelling to localize the subunit using immunofluorescence, due to the relatively low expression of the $\alpha7$ nicotinic receptor subunit in neuronal somata. The combined pharmacological and anatomical data agree with a recent *in situ* hybridization study that showed the presence of $\alpha7$ and $\beta2$ nicotinic receptor subunit mRNAs in all cholinergic neurones and in most GABAergic neurones in the medial septum, and the $\alpha4$ nicotinic receptor subunit mRNA only in non-cholinergic cells (Azam *et al.* 2002). Although the $\alpha7^*$ nicotinic receptor subunit does not require other subunits to form functional ion channels in expression systems, there is evidence that native $\alpha7^*$ nicotinic receptors also contain the $\beta2$ subunit (Khiroug *et al.* 2002). The mRNAs for nicotinic receptor subunits $\alpha3$ and $\beta4$ are evident in moderate levels in the MS/DB (Wada *et al.* 1989; Dineleymiller & Patrick, 1992; Seguela *et al.* 1993), and together with the $\alpha7$, $\alpha4$ and $\beta2$ nicotinic receptor subunits detected there, may account for the variety of nicotinic receptors response types found in the MS/DB.

Muscarinic and nicotinic receptor responses in the MS/DB

In addition to our investigation into the presence of nicotinic receptor responses in the MS/DB, we

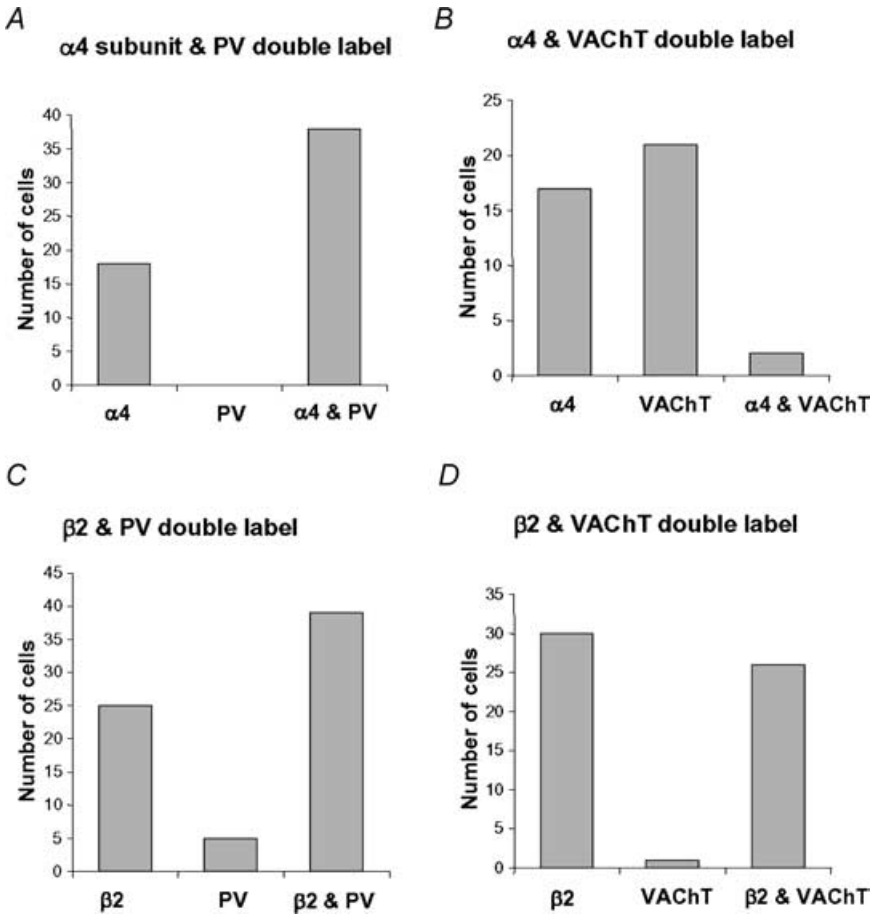

Figure 7. Bar charts showing a quantitative assessment of the double immunofluorescence labelling for the nicotinic receptor subunits $\alpha4$ and $\beta2$, and the neurochemical markers parvalbumin (PV) and VAChT, shown in Figs 5 and 6.

showed that puffed ACh elicits various combinations of muscarinic receptor depolarization and hyperpolarization responses in both GABAergic and cholinergic neurones. No rhythmic burst firing responses were produced with ACh in the MS/DB, whereas such responses have been reported in the lateral septal nucleus (Carette, 1997). Our observations on the muscarinic receptor responses in the MS/DB confirm the findings of a previous report on the MS/DB by Sim & Griffith (1991), which described both hyperpolarization and depolarization responses to bath-applied muscarinic agonists in non-cholinergic cells in the MS/DB. Other *in vitro* studies, on the other hand, have indicated that cholinergic neurones are hyperpolarized by activation of muscarinic receptors, and that GABAergic neurones are depolarized by muscarinic receptor activation (Serafin *et al.* 1996; Liu *et al.* 1998; Wu *et al.* 2003*b*). The reasons for these discrepancies are not clear but could be due to the way that neurones are characterized electrophysiologically by different laboratories. Neuroanatomical studies also have not indicated a selective distribution of muscarinic receptor subtypes in the MS/DB among cholinergic and non-cholinergic neurones (Van der Zee & Luiten, 1994; Levey *et al.* 1995). In conclusion therefore, there is no clear evidence for a segregation of muscarinic receptor subtypes among GABAergic and cholinergic cell types in the MS/DB neurone, suggesting that such an attribute is not critical to the functioning of the MS/DB.

No evidence for fast cholinergic synaptic transmission in the MS/DB

We could not detect the presence of cholinergic synaptic responses in the MS/DB, either in the form of evoked potentials, or spontaneous nicotinic receptor-based synaptic potentials. The MS/DB therefore despite its complement of resident cholinergic neurones, does not depart from the general pattern in the CNS where many neurones generate fast responses to exogenously applied ACh, but few respond to nicotinic synaptic transmission (Alkondon *et al.* 1998; Frazier *et al.* 1998*a*; Hatton & Yang, 2002). There are several explanations for the presence of somato-dendritic receptors in the MS/DB. The first is that they are receptors that are in the process of being transported to the terminals of these neurones, and there is clear evidence that nicotinic receptors exert their influence in the CNS via both presynaptic $\alpha4\beta2^*$ and $\alpha7^*$ nicotinic receptor subtypes (McGehee *et al.* 1995; Clementi *et al.* 2000; Wonnacott *et al.* 2000; Jones *et al.* 2001; Pereira *et al.* 2002). If this were the case, then the cholinergic and GABAergic cells in the MS/DB may possess different types of nicotinic receptor subtypes on their terminals, which could have important functional consequences. The second explanation is that the somato-dendritic nicotinic receptors respond to a 'volume' transmission of ACh. The third possibility is that the nicotinic receptors are localized at GABAergic and glutamatergic postsynaptic sites, as indicated by recent immunocytochemical studies in cortical areas (Fabian-Fine *et al.* 2001; Levy & Aoki, 2002). The implications here are that they are involved in synaptic plasticity because nicotinic receptors, unlike NMDA receptors, do not require the postsynaptic membrane to be depolarized before promoting calcium influx, making them in theory operable at both GABAergic and glutamatergic synapses (Berg & Conroy, 2002). Nicotinic receptors have profound influences on synaptic plasticity in the mesolimbic dopamine system (Dani *et al.* 2001; Mansvelder *et al.* 2002) and hippocampus (Fujii *et al.* 2000), and so may do so in other areas as well.

It will be interesting to determine what role nicotinic receptors play in generation of rhythmic network activity in the MS/DB. Our results indicate that it is unlikely that septal cholinergic cells provide a fast nicotinic excitatory feedback to each other or to neighbouring GABAergic cells during the production of rhythmic activity. Recently we have shown that the frequency of the rhythmic extracellular field activity in the MS/DB slice generated by the bath application 100 nM kainate is modulated by the combined inhibition of nicotinic and muscarinic receptors (H. L. Garner, M. A. Whittington & Z. Henderson, unpublished results). Although in theory the role of presynaptic or somato-dendritic nicotinic receptors in rhythmic activity could be limited by desensitization, this may not be so acute due to the abundance of acetylcholinesterase (AChE) in the CNS. Indeed there is a reasonably good correspondence between the distribution and intensity of histochemical staining for AChE (Shute & Lewis, 1967) and that for the labelling of nicotinic receptors by receptor binding (Clarke *et al.* 1985). The primary role for AChE in the CNS would therefore be to prevent a prolonged desensitization of nicotinic receptors at both presynaptic and postsynaptic sites, rather than to terminate muscarinic transmission. This, combined with the phenomenon of substrate inhibition of AChE, could allow high concentrations of ACh to initially have a strong action on nicotinic receptors before the transmitter becomes rapidly degraded. This would make sense in cases where ACh release is episodic, for example as could occur from cholinergic neurones that are known to display rhythmic burst firing activity during the hippocampal theta rhythm *in vivo* (Brazhnik & Fox, 1997).

Pathological considerations

In our study we showed that $\alpha7^*$ nicotinic receptor subtypes are strongly associated with cholinergic neurones in the MS/DB. This is of interest because basal forebrain cholinergic neurones are susceptible to degeneration in

Alzheimer's disease, and recently it was reported that $A\beta_{1-42}$ selectively binds to the $\alpha7^*$ nicotinic receptor subtype with high affinity (Wang *et al.* 2000*a*,*b*). It has been proposed therefore that the presence of the $\alpha7^*$ nicotinic receptor subtype may be a common factor for selective neuronal pathology in Alzheimer's disease and that it may nucleate Aβ deposition (Dineley *et al.* 2002), or damage neurones after internalization of an $\alpha7^*$ nicotinic receptor–Aβ42 complex (Nagele *et al.* 2002). Nicotine itself seems to have a protective function towards Alzheimer's disease, possibly because it prevents the toxic protein β amyloid from binding to nicotinic receptors (Picciotto & Zoli, 2002). Developing Alzheimer therapies through nicotinic receptor agonists, as an alternative to AChE inhibitors, has therefore become an interesting prospect for pharmaceutical companies.

References

Albuquerque EX, Alkondon M, Pereira EF, Castro NG, Schrattenholz A, Barbosa CT, Bonfante-Cabarcas R, Aracava Y, Eisenberg HM & Maelicke A (1997). Properties of neuronal nicotinic acetylcholine receptors: pharmacological characterization and modulation of synaptic function. *J Pharmacol Exp Ther* **280**, 1117–1136.

Alkondon M, Pereira EF & Albuquerque EX (1998). Alpha-bungarotoxin- and methyllycaconitine-sensitive nicotinic receptors mediate fast synaptic transmission in interneurons of rat hippocampal slices. *Brain Res* **810**, 257–263.

Alonso A, Gaztelu JM, Buno W Jr & Garcia-Austt E (1987). Cross-correlation analysis of septohippocampal neurons during theta-rhythm. *Brain Res* **413**, 135–146.

Amaral DG & Kurz J (1985). An analysis of the origins of the cholinergic and noncholinergic septal projections to the hippocampal formation of the rat. *J Comp Neurol* **240**, 37–59.

Arroyo-Jiménez MD, Bourgeois JP, Marubio LM, Le Sourd AM, Ottersen OP, Rinvik E, Fairén A & Changeux JP (1999). Ultrastructural localization of the α4-subunit of the neuronal acetylcholine nicotinic receptor in the rat substantia nigra. *J Neurosci* **19**, 6475–6487.

Azam L, Winzer-Serhan UH, Chen Y & Leslie FM (2002). Expression of neuronal nicotinic acetylcholine receptor subunit mRNAs within midbrain dopamine neurons. *J Comp Neurol* **444**, 260–274.

Berg DK & Conroy WG (2002). Nicotinic alpha 7 receptors: synaptic options and downstream signaling in neurons. *J Neurobiol* **53**, 512–523.

Bialowas J & Frotscher M (1987). Choline acetyltransferase-immunoreactive neurons and terminals in the rat septal complex: a combined light and electron microscopic study. *J Comp Neurol* **259**, 298–307.

Brashear HR, Zaborszky L & Heimer L (1986). Distribution of GABAergic and cholinergic neurons in the rat diagonal band. *Neuroscience* **17**, 439–451.

Brazhnik ES & Fox SE (1997). Intracellular recordings from medial septal neurons during hippocampal theta rhythm. *Exp Brain Res* **114**, 442–453.

Brazhnik ES & Fox SE (1999). Action potentials and relations to the theta rhythm of medial septal neurons in vivo. *Exp Brain Res* **127**, 244–258.

Carette B (1997). Neurons in the guinea-pig lateral septum generate rhythmic bursting activities *in vitro*, following application of carbachol. *Neurosci Lett* **239**, 93–96.

Celio MR (1990). Calbindin D-28k and parvalbumin in the rat nervous system. *Neuroscience* **35**, 375–475.

Clarke PBS, Schwartz RD, Paul SM, Pert CB & Pert A (1985). Nicotinic binding in rat-brain – autoradiographic comparison of [H-3] acetylcholine, [H-3] nicotine, and [I-125] alpha-bungarotoxin. *J Neurosci* **5**, 1307–1315.

Clementi F, Fornasari D & Gotti C (2000). Neuronal nicotinic receptors, important new players in brain function. *Eur J Pharmacol* **393**, 3–10.

Dani JA, Ji DY & Zhou FM (2001). Synaptic plasticity and nicotine addiction. *Neuron* **31**, 349–352.

Deltoro ED, Juiz JM, Peng X, Lindstrom J & Criado M (1994). Immunocytochemical localization of the alpha-7 subunit of the nicotinic acetylcholine-receptor in the rat central-nervous-system. *J Comp Neurol* **349**, 325–342.

Dineley KT, Xia X, Bui D, Sweatt JD & Zheng H (2002). Accelerated plaque accumulation, associative learning deficits, and up-regulation of alpha 7 nicotinic receptor protein in transgenic mice co-expressing mutant human presenilin 1 and amyloid precursor proteins. *J Biol Chem* **277**, 22768–22780.

Dineleymiller K & Patrick J (1992). Gene transcripts for the nicotinic acetylcholine-receptor subunit, beta4, are distributed in multiple areas of the rat central-nervous-system. *Mol Brain Res* **16**, 339–344.

Dutar P, Lamour Y, Rascol O & Jobert A (1986). Septo-hippocampal neurons in the rat: further study of their physiological and pharmacological properties. *Brain Res* **365**, 325–334.

Fabian-Fine R, Skehel P, Errington ML, Davies HA, Sher E, Stewart MG & Fine A (2001). Ultrastructural distribution of the alpha7 nicotinic acetylcholine receptor subunit in rat hippocampus. *J Neurosci* **21**, 7993–8003.

Frazier CJ, Buhler AV, Weiner JL & Dunwiddie TV (1998*a*). Synaptic potentials mediated via alpha-bungarotoxin-sensitive nicotinic acetylcholine receptors in rat hippocampal interneurons. *J Neurosci* **18**, 8228–8235.

Frazier CJ, Rollins YD, Breese CR, Leonard S, Freedman R & Dunwiddie TV (1998*b*). Acetylcholine activates an alpha-bungarotoxin-sensitive nicotinic current in rat hippocampal interneurons, but not pyramidal cells. *J Neurosci* **18**, 1187–1195.

Freund TF (1989). GABAergic septohippocampal neurons contain parvalbumin. *Brain Res* **478**, 375–381.

Freund TF & Antal M (1988). GABA-containing neurons in the septum control inhibitory interneurons in the hippocampus. *Nature* **336**, 170–173.

Frotscher M & Leranth C (1985). Cholinergic innervation of the rat hippocampus as revealed by choline acetyltransferase immunocytochemistry: a combined light and electron microscopic study. *J Comp Neurol* **239**, 237–246.

Fujii S, Ji ZX & Sumikawa K (2000). Inactivation of alpha 7 ACh receptors and activation of non-alpha 7 ACh receptors both contribute to long term potentiation induction in the hippocampal CA1 region. *Neurosci Lett* **286**, 134–138.

Gloveli T, Dugladze T, Schmitz D & Heinemann U (2001). Properties of entorhinal cortex deep layer neurons projecting to the rat dentate gyrus. *Eur J Neuroscience* **13**, 413–420.

Gorelova N & Reiner PB (1996). Role of the afterhyperpolarization in control of discharge properties of septal cholinergic neurons *in vitro*. *J Neurophysiol* **75**, 695–706.

Green JD & Arduini AA (1954). Hippocampal electrical activity in arousal. *J Neurophysiol* **17**, 533–554.

Griffith WH (1988). Membrane properties of cell types within guinea pig basal forebrain nuclei *in vitro*. *J Neurophysiol* **59**, 1590–1612.

Griffith WH & Matthews RT (1986). Electrophysiology of AChE-positive neurons in basal forebrain slices. *Neurosci Lett* **71**, 169–174.

Harata N, Tateishi N & Akaike N (1991). Acetylcholine-receptors in dissociated nucleus basalis of Meynert neurons of the rat. *Neurosci Lett* **130**, 153–156.

Hatton GI & Yang QZ (2002). Synaptic potentials mediated by alpha 7 nicotinic acetylcholine receptors in supraoptic nucleus. *J Neurosci* **22**, 29–37.

Henderson Z, Harrison PS, Jagger E & Beeby JH (1998). Density of choline acetyltransferase-immunoreactive terminals in the rat dentate gyrus after entorhinal cortex lesions: a quantitative light microscope study. *Exp Neurol* **152**, 50–63.

Henderson Z, Morris NP, Grimwood P, Fiddler G, Yang HW & Appenteng K (2001). Morphology of local axon collaterals of electrophysiologically characterised neurons in the rat medial septal/diagonal band complex. *J Comp Neurol* **430**, 410–432.

Hughes SW, Blethyn KL, Cope DW & Crunelli V (2002). Properties and origin of spikelets in thalamocortical neurones *in vitro*. *Neuroscience* **110**, 395–401.

Jones IW, Bolam JP & Wonnacott S (2001). Presynaptic localisation of the nicotinic acetylcholine receptor beta2 subunit immunoreactivity in rat nigrostriatal dopaminergic neurones. *J Comp Neurol* **439**, 235–247.

Jones GA, Norris SK & Henderson Z (1999). Conduction velocities and membrane properties of different classes of rat septohippocampal neurons recorded *in vitro*. *J Physiol* **517**, 867–877.

Jones S & Yakel JL (1997). Functional nicotinic ACh receptors on interneurones in the rat hippocampus. *J Physiol* **504**, 603–610.

Khiroug SS, Harkness PC, Lamb PW, Sudweeks SN, Khiroug L, Miller NS & Yakel JL (2002). Rat nicotinic ACh receptor alpha 7 and beta 2 subunits co-assemble to form functional heteromeric nicotinic receptor channels. *J Physiol* **540**, 425–434.

King C, Recce M & O'Keefe J (1998). The rhythmicity of cells of the medial septum/diagonal band of Broca in the awake freely moving rat: relationships with behaviour and hippocampal theta. *Eur J Neurosci* **10**, 464–477.

Kiss J, Patel AJ, Baimbridge KG & Freund TF (1990). Topographical localization of neurons containing parvalbumin and choline acetyltransferase in the medial septum-diagonal band region of the rat. *Neuroscience* **36**, 61–72.

Kohler C, Chan-Palay V & Wu JY (1984). Septal neurons containing glutamic acid decarboxylase immunoreactivity project to the hippocampal region in the rat brain. *Anat Embryol* **169**, 41–44.

Lamour Y, Dutar P & Jobert A (1984). Septo-hippocampal and other medial septum-diagonal band neurons: electrophysiological and pharmacological properties. *Brain Res* **309**, 227–239.

Leranth C & Frotscher M (1989). Organization of the septal region in the rat brain: cholinergic-GABAergic interconnections and the termination of hippocampo-septal fibers. *J Comp Neurol* **289**, 304–314.

Levey AI, Edmunds SM, Hersch SM, Wiley RG & Heilman CJ (1995). Light and electron microscopic study of m2 muscarinic acetylcholine receptor in the basal forebrain of the rat. *J Comp Neurol* **351**, 339–356.

Levy RB & Aoki C (2002). Alpha7 nicotinic acetylcholine receptors occur at postsynaptic densities of AMPA receptor-positive and -negative excitatory synapses in rat sensory cortex. *J Neurosci* **22**, 5001–5015.

Lewis PR, Shute CC & Silver A (1967). Confirmation from choline acetylase analyses of a massive cholinergic innervation to the rat hippocampus. *J Physiol* **191**, 215–224.

Liu W, Kumar A & Alreja M (1998). Excitatory effects of muscarine on septohippocampal neurons: involvement of M3 receptors. *Brain Res* **805**, 220–233.

McGehee DS, Heath MJ, Gelber S, Devay P & Role LW (1995). Nicotine enhancement of fast excitatory synaptic transmission in CNS by presynaptic receptors. *Science* **269**, 1692–1696.

McQuiston AR & Madison DV (1999). Nicotinic receptor activation excites distinct subtypes of interneurons in the rat hippocampus. *J Neurosci* **19**, 2887–2896.

Mansvelder HD, Keath JR & McGehee DS (2002). Synaptic mechanisms underlie nicotine-induced excitability of brain reward areas. *Neuron* **33**, 905–919.

Meyer AH, Katona I, Blatow M, Rozov A & Monyer H (2002). In vivo labeling of parvalbumin-positive interneurons and analysis of electrical coupling in identified neurons. *J Neurosci* **22**, 7055–7064.

Milner TA (1991). Cholinergic neurons in the rat septal complex: ultrastructural characterization and synaptic relations with catecholaminergic terminals. *J Comp Neurol* **314**, 37–54.

Morris NP, Harris SJ & Henderson Z (1999). Parvalbumin-immunoreactive, fast-spiking neurons in the medial septum/diagonal band complex of the rat: intracellular recordings *in vitro*. *Neuroscience* **92**, 589–600.

Morris NP & Henderson Z (2000). Perineuronal nets ensheath fast spiking, parvalbumin-immunoreactive neurons in the medial septum/diagonal band complex. *Eur J Neurosci* **12**, 828–838.

Nagele RG, D'Andrea MR, Anderson WJ & Wang HY (2002). Intracellular accumulation of beta-amyloid (1–42) in neurons is facilitated by the alpha 7 nicotinic acetylcholine receptor in Alzheimer's disease. *Neuroscience* **110**, 199–211.

Panula P, Revuelta AV, Cheney DL, Wu JY & Costa E (1984). An immunohistochemical study on the location of GABAergic neurons in rat septum. *J Comp Neurol* **222**, 69–80.

Paxinos G & Watson C (1986). *The Rat Brain in Stereotaxic Coordinates*, 2nd edn. Academic Press, London.

Pereira EF, Hilmas C, Santos MD, Alkondon M, Maelicke A & Albuquerque EX (2002). Unconventional ligands and modulators of nicotinic receptors. *J Neurobiol* **53**, 479–500.

Picciotto MR & Zoli M (2002). Nicotinic receptors in aging and dementia. *J Neurobiol* **53**, 641–655.

Segal M (1986). Properties of rat medial septal neurones recorded *in vitro*. *J Physiol* **379**, 309–330.

Seguela P, Wadiche J, Dineleymiller K, Dani JA & Patrick JW (1993). Molecular-cloning, functional-properties, and distribution of rat brain-alpha-7 – a nicotinic cation channel highly permeable to calcium. *J Neurosci* **13**, 596–604.

Serafin M, Williams S, Khateb A, Fort P & Muhlethaler M (1996). Rhythmic firing of medial septum non-cholinergic neurons. *Neuroscience* **75**, 671–675.

Shute CC & Lewis PR (1967). The ascending cholinergic reticular system: neocortical, olfactory and subcortical projections. *Brain* **90**, 497–520.

Sim JA & Griffith WH (1991). Muscarinic agonists block a late-afterhyperpolarization in medial septum/diagonal band neurons *in vitro*. *Neurosci Lett* **129**, 63–68.

Sorenson EM, Shiroyama T & Kitai ST (1998). Postsynaptic nicotinic receptors on dopaminergic neurons in the substantia nigra pars compacta of the rat. *Neuroscience* **87**, 659–673.

Sotty F, Danik M, Manseau F, Laplante F, Quirion R & Williams S (2003). Distinct electrophysiological properties of glutamatergic, cholinergic and GABAergic rat septohippocampal neurons: Novel implications for hippocampal rhythmicity. *J Physiol* **551**, 927–943.

Stewart M & Fox SE (1990). Do septal neurons pace the hippocampal theta rhythm? *Trends Neurosci* **13**, 163–168.

Sweeney JE, Lamour Y & Bassant MH (1992). Arousal-dependent properties of medial septal neurons in the unanesthetized rat. *Neuroscience* **48**, 353–362.

Van der Zee EA & Luiten PG (1994). Cholinergic and GABAergic neurons in the rat medial septum express muscarinic acetylcholine receptors. *Brain Res* **652**, 263–272.

Wada E, Wada K, Boulter J, Deneris E, Heinemann S, Patrick J & Swanson LW (1989). Distribution of alpha-2, alpha-3, alpha-4, and beta-2 neuronal nicotinic receptor subunit messenger-RNAs in the central nervous-system – a hybridization histochemical-study in the rat. *J Comp Neurol* **284**, 314–335.

Wang HY, Lee DHS, D'Andrea MR, Peterson PA, Shank RP & Reitz AB (2000*a*). beta-amyloid (1–42). binds to alpha 7 nicotinic acetylcholine receptor with high affinity – Implications for Alzheimer's disease pathology. *J Biol Chem* **275**, 5626–5632.

Wang HY, Lee DHS, Davis CB & Shank RP (2000*b*). Amyloid peptide A beta (1–42) binds selectively and with picomolar affinity to alpha 7 nicotinic acetylcholine receptors. *J Neurochem* **75**, 1155–1161.

Wonnacott S, Kaiser S, Mogg A, Soliakov L & Jones IW (2000). Presynaptic nicotinic receptors modulating dopamine release in the rat striatum. *Eur J Pharm* **393**, 51–58.

Wouterlood FG, Bol JGJM & Steinbusch HWM (1987). Double-label immunocytochemistry – combination of anterograde neuroanatomical tracing with phaseolus-vulgaris leukoagglutinin and enzyme immunocytochemistry of target neurons. *J Histochem Cytochem* **35**, 817–823.

Wu M, Hajszan T, Leranth C & Alreja M (2003*a*). Nicotine recruits a local glutamatergic circuit to excite septohippocampal GABAergic neurons. *Eur J Neurosci* **18**, 1155–1168.

Wu M, Newton SS, Atkins JB, Xu CQ, Duman RS & Alreja M (2003*b*). Acetylcholinesterase inhibitors activate septohippocampal GABAergic neurons via muscarinic but not nicotinic receptors. *J Pharm Exp Ther* **307**, 535–543.

Acknowledgements

This work was supported by the Wellcome Trust, Royal Society and the Hungarian Academy of Sciences (OTKA 043170).